Hindawi Publishing Corporation
EURASIP Journal on Wireless Communications and Networking
Volume 2006, Article ID 60585, Pages 1–9
DOI 10.1155/WCN/2006/60585

Joint MIMO-OFDM and MAC Design for Broadband Multihop Ad Hoc Networks

Dandan Wang and Uf Tureli

Electrical and Computer Engineering Department, Stevens Institute of Technology, Hoboken, NJ 07030, USA

Received 1 November 2005; Revised 4 June 2006; Accepted 13 June 2006

Multiple-input multiple-output (MIMO) and orthogonal frequency division multiplexing (OFDM) are very promising techniques to exploit spatial diversity and frequency diversity in the physical layer of broadband wireless communications. However, the application of these techniques to broadband multihop ad hoc networks is subject to inefficiencies since existing medium access control (MAC) schemes are designed to allow only one node to transmit in a neighborhood. Therefore, adding more relays to increase the transmission range decreases the throughput. With MIMO-OFDM, multiple transmissions can coexist in the same neighborhood. A new transceiver architecture with MIMO-OFDM and MAC scheme is proposed in this paper. The new MAC scheme multiple-antennas receiver-initiated busy-tone medium access (MARI-BTMA) is based on receiver-initiated busy-tone medium access (RI-BTMA) and uses multiple out of band busy tones to avoid the collision of nodes on the same channel. With the proposed MAC scheme, multiple users can transmit simultaneously in the same neighborhood. Although basic MARI-BTMA shows good performance at high traffic load, to improve the performance at low traffic loads, 1-persistent MARI-BTMA is proposed so that users can choose different MAC scheme according to the statistical traffic load in the system. In this paper, both theoretical and numerical analysis of the throughput and delay are presented. Analysis and simulation results show the improved performance of MARI-BTMA compared with RI-BTMA and carrier sensing medium access/collision avoidance (CSMA/CA).

1. INTRODUCTION

In the recent years, multihop relaying ad hoc networking has attracted a lot of interest for its flexibility to achieve broad coverage without any infrastructure. Many new techniques have been adopted in ad hoc networks to improve the performance in the physical layer, that is, multiple-input multiple-output (MIMO) and orthogonal frequency division multiplexing (OFDM). MIMO systems take advantage of the spatial diversity obtained by spatially separated antennas in a multipath scattering environment. Several different ways can be used to obtain either a diversity gain to combat signal fading or a capacity gain, that is, space-time coding (STBC) [1], vertical Bell laboratories layered space-time (V-BLAST) [2], and singular value decomposition (SVD) diversity [3]. Thus, MIMO techniques have shown a great potential to improve the capacity of the system in the physical layer [4, 5]. On the other hand, OFDM has become a popular technique for transmission of signals over broadband wireless channels since it provides a very high spectral efficiency, combats multipath fading, and can be simply implemented by fast Fourier transform (FFT) with a low receiver complexity. OFDM has been adopted in several wireless standards such as IEEE 802.11a wireless local area network (WLAN) standard [6] and IEEE 802.16a [7]. For high data-rate transmission, the multipath characteristic of the environment results in a frequency selective MIMO channel. OFDM can transform such a frequency-selective MIMO channel into a set of parallel frequency-flat MIMO channels, and therefore decrease receiver complexity. The combination of MIMO and OFDM can provide higher data rate, reduce the fading of a single link with space-time-frequency codes, mitigate interference by using extra spatial degrees of freedom, and allow simultaneous communication with different nodes using combinations of spatial multiplexing and interference cancellation [7–10].

In this paper, we propose a new transceiver architecture with the capabilities of signal separation and interference cancellation of MIMO-OFDM, in a virtual MIMO scheme combined with OFDM and space-time coding at the transmit nodes. At the receive nodes, multiple antennas are used to separate the independent data flows from different transmit nodes.

This new transceiver architecture allows multiple independent data flows to be transmitted on the same channel simultaneously, which provides the system the capability of multipacket reception (MPR). MPR presents new challenges for medium access control (MAC) in wireless networks since classical MAC schemes are designed to allow only one user in a neighborhood [6, 11–14]. Currently, most research works on MAC schemes with MPR focus on central controlled systems, for example, [15]. However, multihop ad hoc networks lack the aid of central controllers. In the literature, there are several MAC schemes proposed for distributed ad hoc networks. Stream controlled multiple access (SCMA) proposed in [16] can optimize the selection of the streams at the transmit nodes. However, SCMA requires a lot of information exchange between the different nodes. In [17], mitigating interference using multiple antennas MAC (MIMA-MAC) is proposed to mitigate the interference from the neighboring nodes. In the simulation analysis of [17], fairness and throughput are shown improved over the traditional carrier sensing medium access/collision avoidance (CSMA/CA). However, MIMA-MAC inherits the exposed node problem and hidden node problem associated with CSMA/CA [13, 18, 19]. In [19], Tobagi and Kleinrock proposed a busy-tone multiple access (BTMA) to alleviate the hidden problem in a network with a base station. When a base station senses the transmission of a terminal, it broadcasts a busy-tone signal to all terminals, keeping them (except the current transmitter) from accessing the channel. Based on BTMA, Wu and Li proposed the receiver-initiated busy-tone multiple access scheme (RI-BTMA) in [11] for ad hoc networks. The total spectrum resource is divided into two subbands. One is used to transmit busy-tone signals while the other is used to transmit data. The busy tone is used to acknowledge the channel access request and to prevent transmissions from other nodes. It solves the hidden node problem and the exposed node problem. In this paper, based on RI-BTMA, we propose a new MAC protocol multiple-antennas receiver-initiated busy-tone multiple access (MARI-BTMA). MARI-BTMA utilizes multiple busy tones to notify the other nodes of the number of transmissions currently ongoing in the system. To improve the performance at the low traffic load, we also propose 1-persistent MARI-BTMA in this paper. An adaptive scheme is introduced based on the traffic load. Using OFDM in the transceiver architecture, subbands of OFDM signals can be used to transmit busy tones. Therefore, the overhead of busy tones is proportionally small. Performance analysis and simulation results show much better performance than RI-BTMA and CSMA/CA.

The paper is organized as follows. In Section 2, the new transceiver architecture is given. The proposed MAC scheme MARI-BTMA is presented in Section 3. Throughput and delay analysis of MARI-BTMA is given in Section 4. In Section 5, simulation results are given. Conclusions are drawn in Section 6.

2. TRANSCEIVER ARCHITECTURE WITH MIMO-OFDM

In this section, the new transceiver architecture with MIMO-OFDM is presented. Suppose there are six nodes in a network

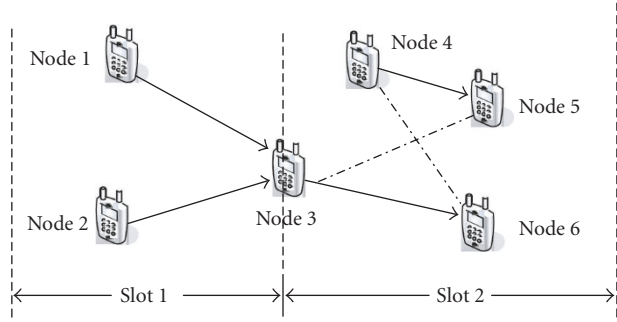

Figure 1: Cooperative network illustration.

shown in Figure 1. Node 3 is the relay node of nodes 1 and 2. The destination of nodes 1 and 2 is node 6. Node 4 has data to send to node 5. In the physical layer, MIMO and OFDM is used to separate signals and cancel interference. Thus, nodes 1 and 2 can transmit to node 3 at the same time by signal separation. The transmission from node 3 to node 6 and the transmission from node 4 to node 5 can also be done simultaneously by interference cancellation. The transceiver architecture in the physical layer with MIMO-OFDM is shown in Figure 2. Suppose each node has n_a antennas. A single space-time (or space-frequency) encoder is employed on these n_a antennas. The space-time encoder takes a single stream of binary input data and transforms it into n_a parallel streams of baseband constellation symbols. Each stream is broken into OFDM blocks. Each OFDM block of constellation symbols is transformed using an inverse fast Fourier transform (IFFT) and transmitted by the antenna for its corresponding stream. Thus, all n_a transmit antennas simultaneously transmit the transformed symbols. At receive nodes, the received signals at each antenna are similarly broken into blocks and processed using an FFT. Then, an interference cancellation scheme is implemented by a space-time processor. The interference cancellation scheme attempts to separate the received signal due to one of the space-time encoders from the received signal due to the other space-time encoder. After this cancellation, maximum-likelihood sequence estimation (MLSE) decoding is employed, followed by successive interference cancellation. The detailed algorithm can be found in [8, 9]. All these algorithms need perfect synchronization. To recover the data flow from independent nodes, the number of transmit nodes must be less than or equal to the number of receive antennas at the receiver nodes. In this paper, we assume that there are two antennas at each node without loss of generality to more than two antennas.

3. MARI-BTMA

In the previous section, multiples nodes were allowed to transmit at the same time thanks to the advanced transceiver architecture in the physical layer. In this section, our proposed MAC protocol—MARI-BTMA—is presented. MARI-BTMA is designed based on the conventional RI-BTMA [11]. In RI-BTMA, the available frequency is divided into two

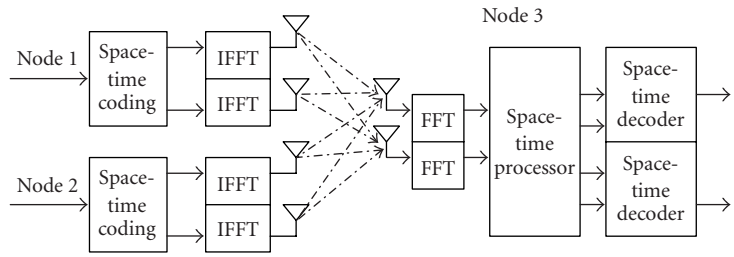

Figure 2: Transceiver scheme with MIMO-STC-OFDM.

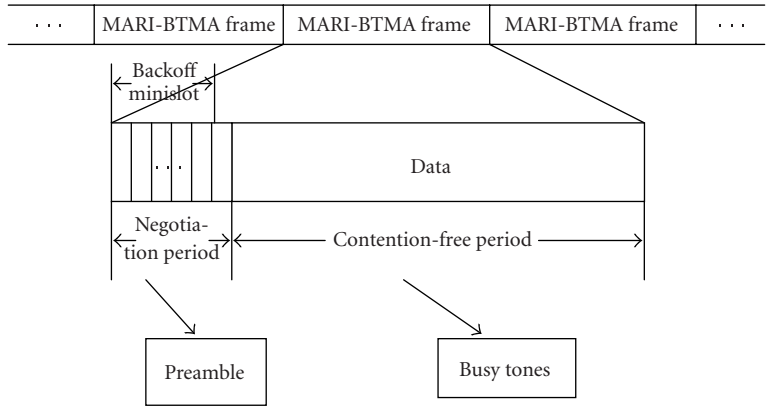

Figure 3: MARI-BTMA frame structure.

parts: control channel and data channel. Busy-tone signals are transmitted on the control channel while data is transmitted on the data channel. When a node has data to transmit, it will first sense the busy-tone channel. If the busy-tone channel is free, a packet of preamble containing the identification of the destination nodes will be sent. Once the preamble is received correctly by the intended receiver, the receiver sets up an out-of-band busy tone and waits for the data packet. The transmitter, upon sensing the busy tone, sends the data packet to the destination. It can be seen that RI-BTMA is designed to accept one user in a neighborhood. To access more than one user, we design a multiple-busy-tone scheme-MARI-BTMA. In MARI-BTMA, the total spectrum resource is divided into several control channels and one data channel. The number of control channels is equal to the number of busy-tone signals and the number of nodes transmitted simultaneously in the system. Since we assume there are two antennas in each node and two independent data flows to separate, two control channels are used in the following. Packet transmissions occur in a frame fashion. The structure of MARI-BTMA is shown in Figure 3. One MARI-BTMA frame is divided into two subframes. One sub frame (contention period) is used to transmit preambles to access the system and the other (contention-free period) is used to transmit data. In the contention period, similar to 802.11 MAC protocol and MIMA MAC in [17], a back off scheme is used to avoid the collision of the preambles sent by more than two nodes in a highly loaded system. The contention period is divided into minislots. The length of each minislot depends on the transmission time and detection delay of the busy tones. The larger size of contention period will reduce the probability of collision of the preambles, while the overhead will be higher. Therefore, the optimal length of contention period should achieve a balance. In the following, we give a detailed description of MARI-BTMA. Since the throughput is not stable when the traffic load is very low shown later in the throughput analysis, we also propose 1-persistent MARI-BTMA and an adaptive MARI-BTMA.

3.1. Basic MARI-BTMA

In the basic MARI-BTMA, only the nodes with data to transmit at the beginning of a frame contend to access the system. A node generating data in the middle of a frame has to wait a random interval till it is scheduled to transmit at the beginning of a frame. Then all the nodes with data to transmit at the beginning of a frame select one minislot in the contention period uniformly and sense the control channels.

(i) If a node senses two busy tones, it will not transmit a preamble in this frame and wait a random interval till it is scheduled to transmit at the beginning of a frame.

(ii) If a node senses one busy tone, it will transmit a preamble. If the preamble is successfully received by the intended receiver, the receiver will set up a busy tone on another free control channel.

(iii) If a node senses no busy tone, it will send a preamble and the receiver will set up a busy tone on either of the control channels once it receives the preamble correctly.

Only the nodes receiving the busy tone from their destination nodes can transmit data in the contention-free period. By sensing the number of busy tones, all the destination nodes get to know how many independent data flows to recover.

3.2. 1-persistent MARI-BTMA

It can be seen that when the traffic load is low, the basic protocol does not work well since all the packets generated during a frame have been ignored. According to [14], when the traffic load is very low, 1-persistent CSMA can improve the throughput of the system greatly. Similar to 1-persistent CSMA, we propose 1-persistent MARI-BTMA in this subsection. In 1-persistent MARI-BTMA, instead of waiting random intervals till the beginning of a frame, all the nodes generating data in the middle of a frame will contend to access the system at the beginning of the next frame. Then all the nodes with data to transmit at the beginning of a frame will get a back off minislot in the contention period and sense the busy-tone channels which is the same with the basic MARI-BTMA.

3.3. Adaptive MARI-BTMA

From the previous two subsections, we know that 1-persistent MARI-BTMA is suitable to the low traffic load, while basic MARI-BTMA is appropriate to the high traffic load. Therefore, in this subsection, we present an adaptive MARI-BTMA to combine the performance of basic MARI-BTMA and 1-persistent MARI-BTMA. In adaptive MARI-BTMA, when the traffic load is low, 1-persistent MARI-BTMA is used while when the traffic load is high, basic MARI-BTMA is adopted. The switch point between 1-persistent scheme and basic scheme depends on the frame length of MARI-BTMA and the traffic load.

4. PERFORMANCE ANALYSIS

In this section, the throughput of MARI-BTMA is analyzed using the method developed by Tobagi and Kleinrock in their study of CSMA and BTMA [18, 19]. The network model consists of a large number of terminals communicating with each other over a single channel. All nodes are within the range of each other. We make the following assumptions for MARI-BTMA protocol and the analysis.

(i) There are N nodes in the system.
(ii) Each node has two antennas. If there are more than two nodes transmitting simultaneously, the receiver cannot recover the original signals correctly. Correspondingly in RI-BTMA, only one node can be accessed in the system, that is, there is no capture effect on the channel.
(iii) Packet collisions are the only source of packet errors.
(iv) The busy-tone signals and the data signals have the same transmission range.
(v) The interference between the busy-tone signals and the data signals is negligible.
(vi) The bandwidth consumption of the busy tones is negligible compared to the bandwidth of the data channel.
(vii) The number of minislots in a contention period is m_1 and the number of minislots in contention-free period is m_2 which is the packet length. Therefore, the frame length is $m_1 + m_2$.
(viii) The arrival of the packets of each node, including newly generated packets and rescheduled packets, constitutes a Bernoulli process with probability p per minislot at each node. Here, the packet will be rescheduled which means that it waits a random interval and tries again.
(ix) The preamble can be successfully received only if there is exactly one preamble transmitted in that minislot.

4.1. Throughput of basic MARI-BTMA

Suppose there are currently M nodes with packets to transmit at the beginning of a frame. These M nodes will first randomly select a minislot in the contention period. Let E_i denote the event that there is only one node choosing the ith minislot, that is, there is no collision in the ith minislot. We call this minislot then "collision-free" minislot. Then the probability of at least one collision-free minislot in all the m_1 minislots in the contention period is

$$
\begin{aligned}
&P_1(m_1, M) \\
&= P\left(\bigcup_{i=1}^{m_1} E_i\right) \\
&= \begin{cases}
\displaystyle\sum_{i=1}^{m_1} P(E_i) - \sum_{i_1<i_2} P(E_{i_1} \cap E_{i_2}) + \cdots \\
\quad +(-1)^{n+1} \displaystyle\sum_{i_1<i_2<\cdots<i_n} P(E_{i_1} \cap E_{i_2} \cdots \cap E_{i_n}) \\
\quad + \cdots + (-1)^{m_1+1} P(E_1 \cap E_2 \cdots \cap E_{m_1}), \qquad m_1 < M, \\
\displaystyle\sum_{i=1}^{m_1} P(E_i) - \sum_{i_1<i_2} P(E_{i_1} \cap E_{i_2}) + \cdots \\
\quad +(-1)^{n+1} \displaystyle\sum_{i_1<i_2<\cdots<i_n} P(E_{i_1} \cap E_{i_2} \cdots \cap E_{i_n}) \\
\quad + \cdots + (-1)^{M+1} P(E_1 \cap E_2 \cdots \cap E_M), \qquad m_1 > M,
\end{cases}
\end{aligned} \tag{1}
$$

$P(E_{i_1} \cap E_{i_2} \cdots \cap E_{i_n})$ is the probability that a specific set of minislots $\{i_1, i_2, \ldots, i_n\}$ is collision-free, that is, each of these n minislots has only one node selecting them. There are $\binom{M}{n} * n! = M!/(M-n)!$ ways of choosing n nodes from M nodes to put in the n minislots without ordering (one minislot is associated with one node). For the left $(M-n)$ nodes, they can be put randomly in the left $m_1 - n$ minislots so that there are $(m_1 - n)^{M-n}$ ways of putting them. Since totally

there are m_1^M ways to put all the M nodes in the m_1 minislots:

$$P(E_{i_1} \cap E_{i_2} \cdots \cap E_{i_n}) = \frac{(M!/(M-n)!)(m_1-n)^{M-n}}{m_1^M}. \tag{2}$$

Therefore,

$$\sum_{i_1<i_2<\cdots<i_n} P(E_{i_1} \cap E_{i_2} \cdots \cap E_{i_n}) = \frac{\binom{m_1}{n}(M!/(M-n)!)(m_1-n)^{M-n}}{m_1^M}. \tag{3}$$

When there are more than two collision-free minislots, only the nodes in the first two collision-free minislots can send preambles since there are at most two busy tones in the system. Let $P_2(M)$ be the probability of one successful preamble transmitted in the contention period. Let $P_3(M)$ be the probability of two successful preambles transmitted in the contention period. Therefore $P_2(M)$ is the probability of only one collision-free minislot in the contention period. $P_3(M)$ is the probability of at least two collision-free minislots in the contention period. The probability that only one minislots is collision-free is equal to the probability that none of the remaining $m_1 - 1$ minislot is collision-free. First, we fix attention on a particular collision-free minislot and a particular node selecting that minislot. $1 - P_1(m_1 - 1, M - 1)$ is the probability that none of the $m_1 - 1$ minislots is collision-free. Then there are $(m_1 - 1)^{M-1}(1 - P_1(m_1 - 1, M - 1))$ ways that only this minislot and this node are collision free. Therefore,

$$P_2(M) = \frac{m_1 M (m_1-1)^{M-1}[1 - P_1(m_1-1, M-1)]}{m_1^M},$$
$$P_3(M) = P_1(m_1, M) - P_2(M). \tag{4}$$

Thus the throughput obtained given M nodes with packets to transmit at the beginning of a frame is

$$S(M) = \frac{P_2(M)m_2 + 2P_3(M)m_2}{m_1 + m_2}. \tag{5}$$

Let X denote the number of packet generated and rescheduled at the beginning of a frame. X is a binomial random variable with parameter N and p. Thus

$$P(X = M) = \binom{N}{M} p^M (1-p)^{N-M}. \tag{6}$$

Therefore, the average throughput of the system is

$$\overline{S} = \sum_{M=1}^{N} P(M)S(M). \tag{7}$$

In the following analysis, we set $m_2 = 100$ and $N = 100$. Figure 4 gives the throughput of basic MARI-BTMA with different contention periods. The throughput of RI-BTMA is also given as a benchmark. In [11], Wu and Li give the calculation of the throughput of RI-BTMA: $\eta = (1 + E(\text{length of data portion}))/(E(X) + E(\text{length of data portion}))$ and $E(X) = 1/P_s$. P_s is the probability of exactly one arrival in the system in a slot. In [11], the preamble is counted as the useful information. However, in this paper, we treat the preamble as overhead, thus the throughput of RI-BTMA is calculated as

$$\overline{S}' = \frac{m_2}{(1/q) + m_2}, \tag{8}$$

where $q = Np(1-p)^{N-1}$.

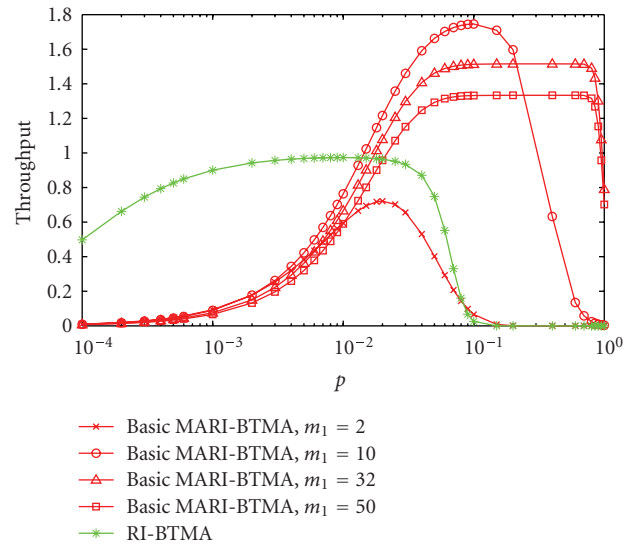

Figure 4: Throughput of basic MARI-BTMA with different contention periods.

Different contention periods correspond to different performance as shown in Figure 4. With an appropriately designed contention period, basic MARI-BTMA is shown to have a much higher throughput than RI-BTMA when the traffic load is high. If the contention period is very short, for example, $m_1 = 2$, the probability that no successful preamble can be transmitted in the contention period will be very high. Thus, the probability that there will be no data transmitted in the contention-free period will be high and the throughput will be reduced. However, if the contention period is very long, for example, $m_1 = 50$, the probability of successful preamble transmitted is high, but the overhead is too high so that the throughput is still low. From Figure 4, we can also see that the higher peak throughput of MARI-BTMA is associated with the unstable situation of the system when the traffic load is very low or very high. One possible solution to this unstable situation is to use 1-persistent MARI-BTMA when the traffic load is very low and a better back off scheme when the traffic load is very high.

4.2. Throughput of 1-persistent MARI-BTMA

Let Y denote the number of packets contending at the beginning of a frame. In 1-persistent MARI-BTMA, Y is a

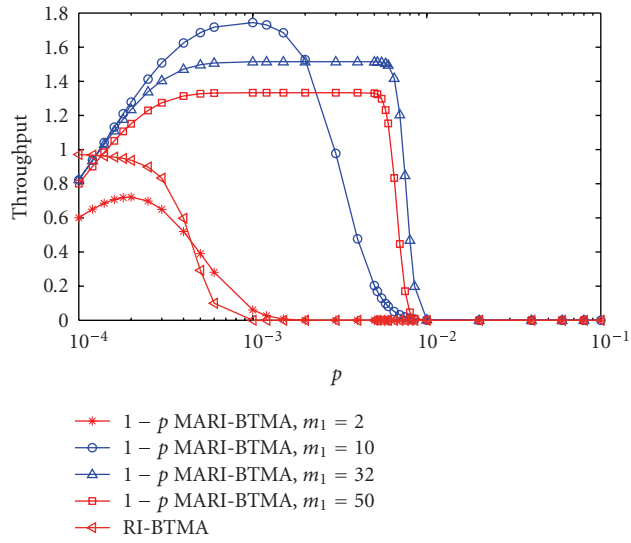

Figure 5: Throughput of 1-persistent MARI-BTMA with different contention periods.

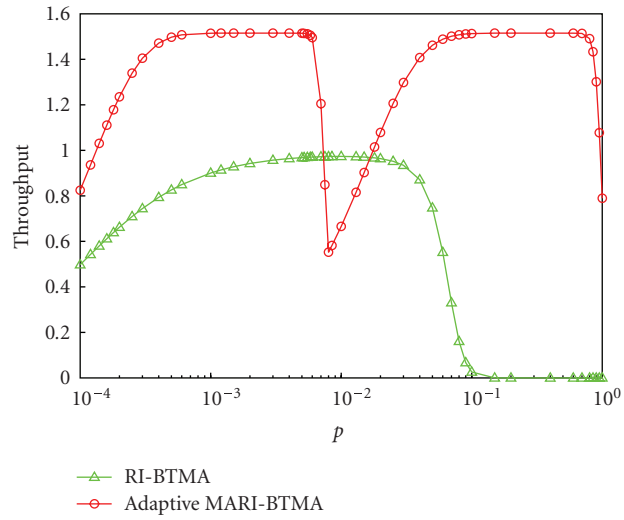

Figure 6: Throughput of adaptive MARI-BTMA.

binomial variable with parameter $N(m_1 + m_2)$ and p:

$$P''(Y = M) = \binom{N(m_1 + m_2)}{M} p^M (1-p)^{N(m_1+m_2)-M}. \tag{9}$$

Thus, the average throughput is

$$\overline{S}'' = \sum_{M=1}^{N(m_1+m_2)} P''(M) S(M), \tag{10}$$

where $S(M)$ is obtained from (5). The throughput of 1-persistent MARI-BTMA is shown in Figure 5.

From it, we can see that 1-persistent MARI-BTMA improves the throughput greatly when the traffic load is very low. However, when the traffic load is high, it goes down very quickly.

4.3. Throughput of adaptive MARI-BTMA

From the previous Sections 4.1 and 4.2, we know that 1-persistent MARI-BTMA works very well at the low traffic load while basic MARI-BTMA works very well at the high traffic load. In this subsection, we investigate the performance of the system using adaptive MARI-BTMA. We set $m_1 = 32$, $m_2 = 100$, and $N = 100$. From Figures 4 and 5, we know the cross point of basic MARI-BTMA and 1-persistent MARI-BTMA is $p = 0.01$. Therefore, we select $p = 0.01$ as the switch point between 1-persistent scheme and basic scheme, that is, when the statistic packet generation probability is less than 0.01, 1-persistent scheme is used. However, if that probability is larger than 0.01, basic MARI-BTMA is used. Figure 6 shows the performance of adaptive MARI-BTMA.

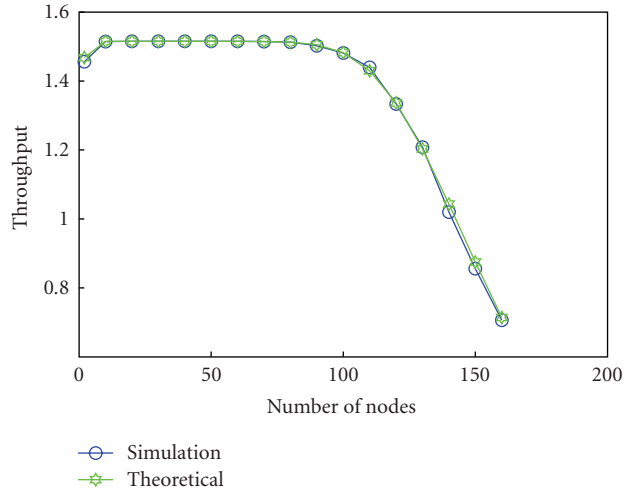

Figure 7: Saturation throughput of MARI-BTMA.

4.4. Saturation throughput analysis

In this subsection, the saturation throughput of basic MARI-BTMA is analyzed. The saturation throughput is obtained when all the N nodes in the system always have data to transmit. In Section 4.1, if $p = 1$, it is in the saturation situation. Thus, the saturation throughput (ST) is

$$\mathrm{ST} = \frac{P_2(N)m_2 + 2P_3(N)m_2}{m_1 + m_2}. \tag{11}$$

In Figure 7, both the theoretical result from (11) and simulation results are given when $m_1 = 32$ and $N = 50$. From Figure 7, we can see that simulation results and theoretical results match very well. The slight difference is caused by the limited number of iterations in simulation. Compared with

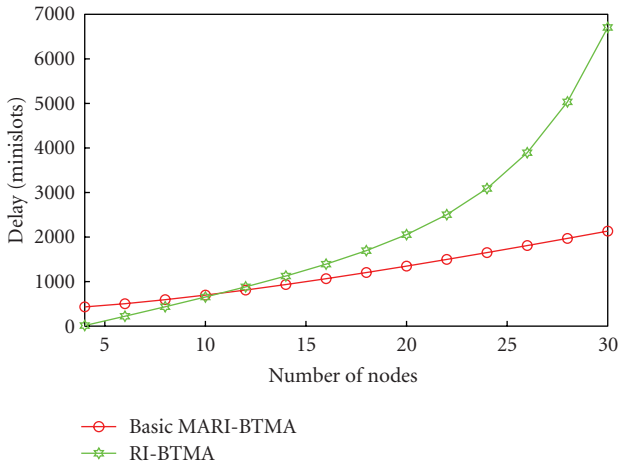

Figure 8: Delay performance of MARI-BTMA and RI-BTMA.

the saturation throughput of 802.11 given by [13], which is around 0.9 with the same windows length (32) and the number of nodes (50), the saturation throughput of MARI-BTMA is much higher, around 1.5.

4.5. Delay performance of MARI-BTMA

In this subsection, the delay performance of basic MARI-BTMA is given. Similar to the delay performance of slotted Aloha given in [14], we can get the average delay

$$D = 1 - \frac{1}{p} + \frac{N}{\overline{S}}, \tag{12}$$

where p is the transmission probability, N is the number of nodes in the system, and $\overline{S}$ is the throughput from (7). The average delay obtained from (12) is the average number of frames back logged. If we calculate in minislots, the average delay is

$$D = (m_1 + m_2) * \left(1 - \frac{1}{p} + \frac{N}{\overline{S}}\right). \tag{13}$$

Similarly, the average delay of basic RI-BTMA is

$$D = (1 + m_2) * (1 - 1/p + N/\overline{S}'), \tag{14}$$

where $\overline{S}'$ is calculated from (8). The relation between delay and number of nodes is given in Figure 8. It can be seen from Figure 8 that delay increases with the increasing of the number of nodes in the system and the delay of MARI-BTMA is much less than that of RI-BTMA.

5. SIMULATION RESULTS

In this section, two scenarios are expressed to compare the performance of the new MAC scheme with the traditional CSMA/CA and RI-BTMA. In the first scenario, the effect of physical layer to the throughput is considered. For the second scenario, we only consider the effect of MAC to the throughput, that is, the collision of more than two packets is the only source of packet error. All the simulations are run in MATLAB.

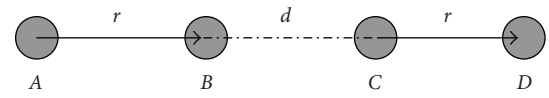

Figure 9: Simulation topology 1.

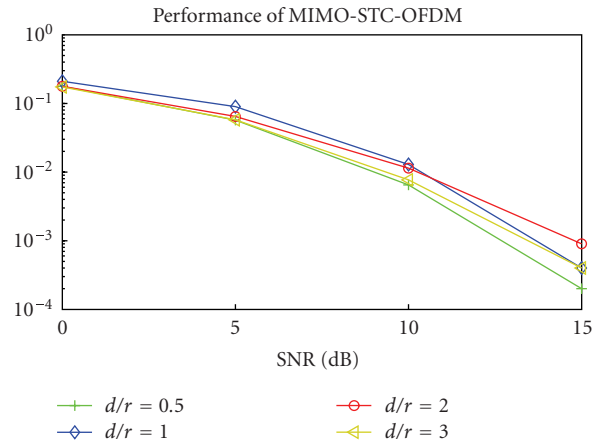

Figure 10: Physical layer performance.

5.1. Simulation scenario 1

In this subsection, simulation results are given both in the physical layer and MAC layer. We use the same simulation scenario in [17] shown in Figure 9. Node A has constant data packets to transmit to node B. Node C has constant data packets to transmit to node D. The distances between A and B, C, and D are fixed, while the distance between B and C can be changed. For the distances in the simulation, the relative distances are used.

5.1.1. Physical layer performance

In this paper, to simplify the simulation, we use Alamouti space-time coding at the transmitter. At the receiver, we use the signal separation algorithm described in [9]. Improved space-time or space-frequency coding and space-time processors can be used in this scheme directly. Figure 10 gives the performance of packet error rate (PER) versus signal-to-noise-ratio (SNR). In the simulation, all the antennas at the transmitter nodes have the same power. A 4-tap frequency selective channel model is used with the variance equal to the path loss $(1/d^4)$. The channel information is assumed to be known at the receiver side.

5.1.2. MAC layer performance evaluation

In this subsection, the normalized throughputs of CSMA/CA and MARI-BTMA are given. The input signal-to-noise ratio

Table 1: Comparison of throughput of CSMA/CA and MARI-BTMA.

			$D/r = 0.5$	$D/r = 1$	$D/r = 2$	$D/r = 3$
CSMA/CA	Access probability	User1	0.5	0.5	1	1
		User2	0.5	0.5	1	1
	PER	User1	0.0075	0.0075	0.0566	0.0164
		User2	0.0075	0.0075	0.01	0.0082
	Throughput	User1	0.4963	0.4963	0.9434	0.9836
		User2	0.4963	0.4963	0.99	0.9918
MARI-BTMA	Access probability	User1	1	1	1	1
		User2	1	1	1	1
	PER	User1	0.0077	0.0188	0.0566	0.0164
		User2	0.0263	0.0566	0.01	0.0082
	Throughput	User1	0.9021	0.892	0.8576	0.8942
		User2	0.8852	0.8576	0.9	0.9016

is 15 dB. The carrier sensing radius is 1.5. The detection radius of RTS and CTS is 1.1. The busy-tone sensing radius is 1.5. Packet error rate (PER) is used in the calculation of throughput. In this simulation, 1/2 rate convolution channel coding is used. Throughput is calculated as

$$S = (1 - \text{PER}) * \frac{\text{number of accessed packets}}{\text{total number of packets}} * \frac{m_2}{m_1 + m_2}. \tag{15}$$

In the simulation, $m_1 = 10$ and $m_2 = 100$. For CSMA/CA, we ignore the overhead of RTS/CTS.

From Table 1, we can see that when node B and node C are close to each other, only one node is accessed with CSMA/CA. However, with MARI-BTMA, both nodes can access to the system. When node B and node C are far away, for example, larger than 1.5, CSMA/CA and MARI-BTMA both guarantee the access of these two nodes. However, for the reason of the fixed structure, the overhead of MARI-BTMA is slightly higher than CSMA/CA. It is interesting to point out that since PER is in the level of 10^{-2}, it is access control probability which dominates the throughput.

5.2. Simulation scenario 2

In the above subsection, we can see that MARI-BTMA works well in the simple scenario. In this subsection, we will see that MARI-BTMA also works well in a scalable system. In the simulation scenario given in Figure 11, Node B to node A, node C to node A, node D to node E, node H to node E, and node G to node F have constant data flows to transmit. All the nodes have the same distance r with each other. The carrier sensing range is r. The lengths of both contention period are 32 minislots.

Simulation results are given in Table 2. It can be seen from Table 2 that MARI-BTMA can get better performance than MIMA in [17] and much higher throughput than RI-BTMA and CSMA/CA. The problem with MIMA is that it has hidden node problems and exposed node problems associated with CSMA/CA which cause MIMA to have high overhead. Therefore, even though MIMA can access two users simultaneously, its throughput is still less than RI-BTMA.

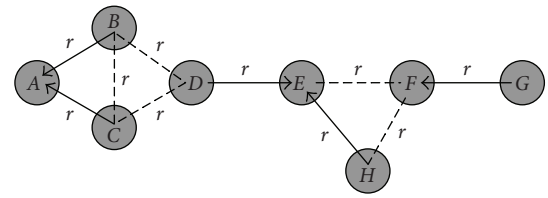

Figure 11: Simulation topology 2.

Table 2: Comparison of throughput.

	MARI-BTMA	RI-BTMA	CSMA/CA	MIMA
Throughput	0.68	0.59	0.35	0.55

6. CONCLUSION

In this paper, we propose a new transceiver architecture with MIMO-OFDM in the physical layer and MARI-BTMA in the MAC layer. MARI-BTMA uses multiple out of band signals busy tones to notify the number of users in the system so that to avoid the collision of the nodes on the same channel. In MARI-BTMA, the packet slot is divided into two subframes: contention subframe and contention-free subframe. The contention sub frame is used to access the nodes, while the contention-free sub frame is used to transmit data for the successfully accessed nodes. Two MARI-BTMA protocols are proposed in this paper. One is basic MARI-BTMA which is suitable to moderate traffic load. The other is 1-persistent MARI-BTMA which is used in the system with low traffic load. By combining basic MARI-BTMA and 1-persistent MARI-BTMA, an adaptive MARI-BTMA is proposed. The throughput analysis of basic MARI-BTMA, 1-persistent MARI-BTMA, and adaptive MARI-BTMA as well as the delay performance of the basic MARI-BTMA are given in this paper. From both the theoretical analysis and simulation results, the performance of MARI-BTMA is shown to be much better than that of CSMA/CA, RI-BTMA or MIMA.

ACKNOWLEDGMENTS

This work was supported in part by the US Army Contract WI5QKN-05-p-0261, AFOSR Grant FA9550-05-1-0329, and NSF Grant CNS-0520232.

REFERENCES

[1] V. Tarokh, H. Jafarkhani, and A. R. Calderbank, "Space-time block codes from orthogonal designs," *IEEE Transactions on Information Theory*, vol. 45, no. 5, pp. 1456–1467, 1999.

[2] G. D. Golden, C. J. Foschini, R. A. Valenzuela, and P. W. Wolniansky, "Detection algorithm and initial laboratory results using V-BLAST space-time communication architecture," *Electronics Letters*, vol. 35, no. 1, pp. 14–16, 1999.

[3] J. Ha, A. N. Mody, J. H. Sung, J. R. Barry, S. W. McLaughlin, and G. L. Stüber, "LDPC coded OFDM with alamouti/SVD diversity technique," *Wireless Personal Communications*, vol. 23, no. 1, pp. 183–194, 2002.

[4] A. Goldsmith, S. A. Jafar, N. Jindal, and S. Vishwanath, "Capacity limits of MIMO channels," *IEEE Journal on Selected Areas in Communications*, vol. 21, no. 5, pp. 684–702, 2003.

[5] S. Vishwanath, N. Jindal, and A. Goldsmith, "On the capacity of multiple input multiple output broadcast channels," in *IEEE International Conference on Communications (ICC '02)*, vol. 3, no. 3, pp. 1444–1450, New York, NY, USA, April-May 2002.

[6] "IEEE Standard for Wireless LAN Medium Access Control (MAC) and Physical Layer (PHY) Specifications," November 1997. P802.11.

[7] H. Yang, "A road to future broadband wireless access: MIMO-OFDM-based air interface," *IEEE Communications Magazine*, vol. 43, no. 1, pp. 53–60, 2005.

[8] Y. Li, J. H. Winters, and N. R. Sollenberger, "Signal detection for MIMO-OFDM wireless communications," in *IEEE International Conference on Communications (ICC '01)*, vol. 10, pp. 3077–3081, Helsinki, Finland, June 2001.

[9] R. S. Blum, Y. Li, J. H. Winters, and Q. Yan, "Improved space-time coding for MIMO-OFDM wireless communications," *IEEE Transactions on Communications*, vol. 49, no. 11, pp. 1873–1878, 2001.

[10] A. Stamoulis, S. N. Diggavi, and N. Al-Dhahir, "Intercarrier interference in MIMO OFDM," *IEEE Transactions on Signal Processing*, vol. 50, no. 10, pp. 2451–2464, 2002.

[11] C. Wu and V. O. K. Li, "Receiver-initiated busy-tone multiple access in packet radio networks," in *Proceedings of the ACM Workshop on Frontiers in Computer Communications Technology (SIGCOMM '87)*, pp. 336–342, Stowe, Vt, USA, August 1987.

[12] Z. J. Haas and J. Deng, "Dual busy tone multiple access (DBTMA) - a multiple access control scheme for ad hoc networks," *IEEE Transactions on Communications*, vol. 50, no. 6, pp. 975–985, 2002.

[13] G. Bianchi, "Performance analysis of the IEEE 802.11 distributed coordination function," *IEEE Journal on Selected Areas in Communications*, vol. 18, no. 3, pp. 535–547, 2000.

[14] R. Rom and M. Sidi, *Multiple Access Protocols Performance and Analysis*, Springer, New York, NY, USA, 1990.

[15] Q. Zhao and L. Tong, "A multiqueue service room MAC protocol for wireless networks with multipacket reception," *IEEE/ACM Transactions on Networking*, vol. 11, no. 1, pp. 125–137, 2003.

[16] K. Sundaresan, R. Sivakumar, M. A. Ingram, and T.-Y. Chang, "Medium access control in ad hoc networks with MIMO links: optimization considerations and algorithms," *IEEE Transactions on Mobile Computing*, vol. 3, no. 4, pp. 350–365, 2004.

[17] T. Tang, M. Park, R. W. Heath Jr., and S. M. Nettles, "A joint MIMO-OFDM transceiver and MAC design for mobile ad hoc networking," in *International Workshop on Wireless Ad-Hoc Networks (IWWAN '04)*, pp. 315–319, Oulu, Finland, May-June 2004.

[18] L. Kleinrock and F. A. Tobagi, "Packet switching in radio channels—1. Carrier sense multiple-access modes and their throughput-delay characteristics," *IEEE Transactions on Communications*, vol. 23, no. 12, pp. 1400–1416, 1975.

[19] F. A. Tobagi and L. Kleinrock, "Packet switching in radio channels—2. The hidden terminal problem in carrier sense multiple-access and the busy-tone solution," *IEEE Transactions on Communications*, vol. 23, no. 12, pp. 1417–1433, 1975.

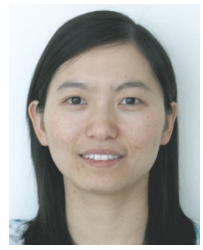

Dandan Wang received the B.S. and M.S degrees in electrical engineering from Beijing University of Posts and Telecommunications, Beijing, China, in 2000 and 2003, respectively. She worked at China Radio Research Lab, Ericsson, from 2003 to 2004. From August 2004 to August 2005, she was with Department of Electrical and Computer Engineering, Stevens Institute of Technology, Hoboken, New Jersey. She is currently a Ph.D. student at the Department of Electrical and Computer Engineering, University of Texas at Dallas. Her research interests include wireless communications and networking, signal processing for communications, and sensor networks.

Uf Tureli received the B.S. degree in 1994 from Bogazici University, Istanbul, Turkey, and the M.S. and Ph.D. degrees in 1998 and 2000, respectively, from the University of Virginia, Charlottesville, all in electrical engineering. Since July 2000, he has been an Assistant Professor at the Department of Electrical and Computer Engineering, Stevens Institute of Technology, Hoboken, New Jersey. He is the Director of the Wireless Research Laboratory at the Department of Electrical and Computer Engineering and Associate Director of Wireless Network Security Center (WiNSeC) at Stevens Institute of Technology. His research interests include signal processing with application to broadband wireless networks, estimation and detection for scalable, adaptive, and robust communications and propagation studies. He has published numerous journal and conference articles in detection and estimation for scalable, adaptive, and robust broadband wireless communications.